Journal of Neonatal Surgery
ISSN(Online): 2226-0439
Vol. 14, Issue 13s (2025)
https://www.jneonatalsurg.com

OPEN ACCESS

Development and Characterization of Copper Oxide and Copper-Zinc Oxide Nanoparticles Synthesized Using Moringa oleifera: Photocatalytic and Antibacterial Applications

Abhay Thakur[1], Rolika Gupta[2], Shriyanshu Thakur[3], Shivam Sharma[4], Sahil Thakur[1], Anjana Devi[*5]

[1]Research Scholar, Department of Pharmacy, Career Point University, Hamirpur, (H.P)-176041
[2]Assistant Professor, Division of Microbiology, Career Point University, Hamirpur, (H.P)-176041
[3]Research Scholar, Division of Microbiology, Career Point University, Hamirpur, (H.P)-176041
[4]Research Scholar, Division of Botany, Career Point University, Hamirpur, (H.P)-176041
[5]Associate Professor, Department of Pharmacy, Career Point University, Hamirpur (H.P)-176041

***Corresponding Author:**
Dr. Anjana Devi
Associate Professor, Department of Pharmacy, Career Point University, Hamirpur (H.P)-176041
Email ID: anjana.pharmacy@cpuh.edu.in

Cite this paper as: Abhay Thakur, Rolika Gupta, Shriyanshu Thakur, Shivam Sharma, Sahil Thakur, Anjana Devi, (2025) Development and Characterization of Copper Oxide and Copper-Zinc Oxide Nanoparticles Synthesized Using Moringa oleifera: Photocatalytic and Antibacterial Applications. *Journal of Neonatal Surgery*, 14 (13s), 388-397.

ABSTRACT

The Study synthesizes and characterizes environmentally friendly synthesized copper oxide (CuO) and copper-zinc oxide (CuZnO) nanoparticles using extract from Moringa oleifera. Their optical antibacterial structural morphological photocatalytic properties were systematically studied for the precipitation method synthesis of nanoparticles. Fourier-transform infrared spectroscopy (FTIR) was conducted to ensure the presence of active biomolecules which could stabilize the nanoparticles, while the X-ray diffraction (XRD) analysis confirmed the crystalline nature of the synthesized nanoparticles. The spheroidal morphology was confirmed by scanning electron microscopy (SEM) and transmission electron microscopy (TEM) and revealed that CuZnO showed more uniform dispersion with less agglomeration compared with CuO. Escherichia coli was used to measure the antibacterial activity of CuO and CuZnO nanoparticles by the agar well diffusion method. The results showed that CuZnO exhibited greater antibacterial activity by synergetic effect between copper ions and zinc ions. In the photocatalytic experiment, it has also shown that CuZnO nanoparticles significantly improved the degradation efficiency of Malachite Green (MG) dye, with 95% degraded under UV light irradiation. Degradation kinetics pseudo-first-order model, and the degradation rate exhibited a direct proportion relation to the concentration of catalyst. These findings suggest that CuO and CuZnO nanoparticles may be promising candidates for environmental remediation and biomedical applications. Due to their multifaceted features, high stability, and Benign synthesis environment, they are good candidates for antimicrobial coatings, wastewater treatment, and several nanotechnology applications. In future studies, focus should be placed on application, scalability, and functional property enhancement.

Keywords: *Green Synthesis, Copper Oxide Nanoparticles, Copper Zinc Oxide Nanoparticles, Moringa oleifera, Antibacterial Activity, Photocatalysis*

1. INTRODUCTION

Nanotechnology is the name given for technology applied to atoms or molecules at the nanoscale (1–100 nm) (1, 2). The most basic feature of nano particles is, that it occupies a greater number of atoms in them. (3,4) Due to their negative environmental impacts, the chemical and physical processes used to produce nanoparticles are not very practical. So, scholars avoid this approach. Recently, the green synthesis approach is being employed for synthesizing nanoparticles (5,6). Green synthesis is safer, less harmful to the environment, simple, and energy and time efficient with high yields. (7) NiO, CuO, ZnO, MgO are examples of metal oxide nanoparticles, having been produced by physical, chemical, and biological methods. They consist of widely used semiconductors with a variety of uses, like Fe2O3 nanoparticles. Another area to which iron oxide nanoparticles have been utilized since 1990 is photocatalysis, biotechnology, medicine and the environment. (8) This NPs have a strong antibacterial effect mainly through interaction with bacterial DNA and destruction of the plasma membrane of gram-negative bacteria. (9) Doping involves the precise modification of material properties by the insertion of ions into the crystal framework of metal oxides, enhancing their electrical, optical, and catalytic

performances. Cu-NPs are highly reactive and can be used in biological, catalytic, and antibacterial applications due to their high surface-to-volume ratios. (11). Cu-NPs work well against drug-resistant bacteria because they can break down the bacterial cell membrane and generate reactive oxygen species (ROS), which kills the bacteria. A similar way, ZnO-NPs have high anti-bacterial potency, ultraviolet (UV) filter capability and good biocompatibility, which is being used in healthcare, environment and optoelectronics. (12) Metals such as $Cu2^{+}$, $Mn2^{+}$, and $Ga2^{+}$ could be used to dope ZnO-NPs to increase photocatalytic efficiency and minimize electron-hole recombination. These metals are used in gas sensors, solar cells and medicinal coatings. (13). Moringa oleifera, commonly known as the drumstick tree, is a very valuable plant for both food and medicine. Its anti-inflammatory, antibacterial, and antioxidant qualities are attributed to its abundance of minerals (calcium, iron, potassium, zinc), vitamins (A, C, and E), and bioactive substances (phenolic acids and flavonoids). (14) Strong antioxidants included in the leaves, including as quercetin and chlorogenic acid, aid in lowering oxidative stress, which has been connected to long-term conditions like diabetes and heart disease. (15) The antibacterial properties of these seeds produce bioactive peptides (responsible for the removal of bacterial contaminants) making them popular in water treatment methods. (16) Antifungal, anticancer and antibacterial properties of Cu-NPs have been reported as well through Green-synthesised Cu-NPs from Moringa oleifera have the ability to act as stabilizing and reducing agents. Their safe use in humans requires appropriate processing and dosage because certain components include chemicals (alkaloids) that can be toxic if used excessively. (17).

2. MATERIAL AND METHODS

The selected plant material was gathered from Hamirpur, India, and verified by the Botany Division of Career Point University, Hamirpur. Double-distilled water was used to thoroughly wash the chosen plant's leaves to get rid of dust and other impurities. Trihydrate of copper nitrate (Cu (NO3)2). Copper (II) nitrate trihydrate [Cu (NO3)2.3H2O], zinc nitrate hexahydrate (Zn (NO3)2.6H2O), ethanol, sodium hydroxide (NaOH), and Mueller Hinton agar (found in our research lab) were among the materials used in this experiment. Every piece of glassware utilized in these investigations is dried in a hot air oven after being carefully cleaned with chromic acid.

Extraction forms the leaf of *Moringa oleifera*

The Moringa oleifera plant's leaves are extracted using Soxhlet extraction. Step 1: The cleaned leaves of the chosen plant were allowed to air dry for approximately 15 days at room temperature. A mortar and pestle are then used to grind the dried leaves into a coarse powder. After wrapping 100g of the leaf powder in muslin cloth and moving it to the Soxhlet device, 500 ml of ethanol was added to a round-bottom flask, which was then put within the Soxhlet assembly. About 60°C is the constant temperature in the Soxhlet assembly. (18) This method extracts leaf extract by using ethanol as a solvent. After extracting leaves three and four in terms of cycles, then one-third of the ethanol is extracted. Stripping ethanol is done by a condensation method. Qualitative Phytochemical Screening of Leaf Extract: The leaf extract was screened for phytochemical using standard methods. (19) and the result is shown in Table 1.

Table no 1. Phytochemical Study of the Leaf Extract of Moringa oleifera

S. No	Different Phytoconstituents	Ethanolic Leaf Extract
1	Alkaloids	Presence
2	Steroids	Presence
3	Flavonoids	Presence
4	Tannins	Presence
5	Coumarins	Absence
6	Saponins	Presence
7	Terpenoids	Presence
8	Phenols	Presence
9	Glycosides	Presence
10	Anthraquinones	Absence
11	Cardiac Glycosides	Presence
12	Carotenoids	Presence
13	Proteins & Amino Acids	Presence

Because of some identified scientific studies that demonstrate the smaller particle size of the nanoparticles synthesized using dried leaf extract compared to the synthesized fresh leaf extract, as well as the fact that the antioxidant activity of the dried leaf was higher than that of the fresh leaf, dried leaf extract is frequently used in the preparation of nanoparticles.

2.1 Green synthesis of CuO NPs and CuZnO NPs

2.1.1 Synthesis of copper oxide nanoparticles:

CuO nanoparticles were made by dissolving 2.416 grams of copper metal in 100 millilitres of distilled water in a beaker. The temperature was kept at 75 °C using a thermometer, and the beaker was set up on a magnetic stirrer that was set to agitate at 300–500 RPM. To guarantee total dissolution, the solution was constantly agitated for an hour. The bio reduction process was then accelerated by adding 10 mL of Moringa oleifera extract and stirring the mixture for an additional hour. Four grams of NaOH were dissolved in thirty millilitres of distilled water, and the solution was then added dropwise from a burette while spinning to the PH. Using a pH paper, the solution's pH was measured and set to 11. For four to five hours, the reaction mixture was constantly stirred. CuO nanoparticles formed when the solution was allowed to cool to room temperature (after stirring was finished). The produced nanoparticles were cleaned three or four times using distilled water to get rid of impurities. In a vacuum oven, the cleaned nanoparticles were dried for 24 hours at 50–60°C. The dried nanoparticles were collected using a micro spatula and put into a sample tube for additional examination. (20,21).

2.1.2 Synthesis of copper Zinc oxide nanoparticles

CuZnO NPs were prepared using a 90:10 copper to zinc molar ratio, where the amounts of copper and zinc used were 2.367 g and 0.059 g, respectively. For complete dissolution, the metal salts are dissolved separately in different beakers containing 50 millilitres of distilled water and stirred (300-500 RPM) for 20 to 30 minutes. After thoroughly mixing the two solutions, they were moved into a beaker and stirred with a magnetic stirrer to distribute them equally. After stirring to keep the reaction at 75 °C, NaOH was added to the solution drop by drop until the pH was brought down to 11. The reaction was continued for four to five hours with constant stirring. Afterwards, to eliminate any remaining unreacted materials, Prior to repeatedly washing the produced NPs with distilled water, the solution was allowed to get to room temperature. After being purified with hot water, the produced nanoparticles were dried in a vacuum oven for 24 hours at 50–60 °C. The dried CuZnO nanoparticles were then gathered and stored in a sample tube for later use and analysis.

2.2 Characterization of the nanoparticles

Several analytical methods are used to characterize CuO and CuZnO nanoparticles. The several spectroscopic techniques' underlying principles are as follows:

2.2.1 X-Ray Diffraction

One analytical method for determining the crystalline nature of a sample is X-ray diffraction (XRD). To ascertain the contaminants and crystalline quality of the produced nanoparticles, we are using a Rigaku X-ray diffractometer.

2.2.2 Ultraviolet-visible spectroscopy

Synthesized copper oxide and copper zinc oxide nanoparticles are detected using UV-Vis spectroscopy. We identified the peak at several wavelengths using a UV-Vis Spectrophotometer.

2.2.3 Fourier Transform infrared spectroscopy

Thermo Scientific's FTIR Spectroscopy is mostly utilized to identify the functional group that is present in the produced nanoparticles. The FTIR spectrophotometer has a scanning range of 400 cm-1 to 4000 cm-1.

2.2.4 Scanning Electron Microscopy

This technique creates an image of the sample by scanning it with an electron focus beam. These include details regarding the topography, morphology, and surface of the sample. SEM (Zeiss evo-18) is mostly used to determine the material's surface morphology.

2.2.5 Transmission electron microscopy

TEM reveals atomic-level structures by transmitting electrons through ultrathin materials to generate high-resolution images. The produced nanoparticles' size, shape, and morphology were examined using HR-TEM (Tecnai G2 20 S-TWIN) from Thermo Fisher at 200 kV. To help with nanoparticle characterization for a variety of applications, SAED patterns verified crystallinity and ImageJ software calculated the mean particle size.

2.3 Antibacterial activity

The antibacterial activity (AA) of green-synthesised copper oxide (CuO) and copper zinc oxide (CuZnO) species nanoparticles against Escherichia coli (E. coli) was assessed using the Agar well diffusion method. Strains of bacteria were put into nutrient broth, which was then incubated for 24 hours at 37°C to create bacterial cultures. CuO and CuZnO nanoparticle stock solutions (5, 10 and 20 mg/mL) were dissolved in distilled water and ultrasonicated for 30 minutes. Mueller-Hinton agar (MHA) plates were inoculated with sterile swabs, followed by the creation of wells (diameter 6–8 mm) using a cork borer. To ascertain each plate's zones of inhibition (ZOI), pure water was added to the control well and progressively higher concentrations of the nanoparticle solutions were applied well-wise on the other plates. The plates were then incubated for 24 hours at 37°C. It should be noted that CuZnO exhibited greater antibacterial activity than CuO;

this could be because copper and zinc work in concert to increase the antibacterial activity. The results show that green-synthesized CuO and CuZnO nanoparticles are potential environmental helpful antibacterial agents.

2.4 Photocatalytic activity

CuO and CuZnO NPs were investigated for their photocatalytic activity under a UV source; and the MG dye was used as test substance. The room where they set up the experiment apparatus was dark. 100 ml of a dye solution containing 10 ppm MG was used with 25, 50, and 100 mg of CuO and CuZnO NPs in each experiment. This mixture was then exposed to UV radiation for approximately 80 minutes to break it down. Absorbance of MG dye at lambda = 631 was determined using a UV-visible instrument every 10 minutes to find the degradation rate.

3. RESULTS AND DISCUSSION

A high content of various phytochemicals in Moringa oleifera make the leaf extract suitable for both reducing and stabilizing agent for CuO and CuZnO nanoparticles. Their removal from the leaves using the Soxhlet extraction procedure facilitated the environmentally friendly production of nanoparticles. The co-precipitation method based on mixing the Moringa oleifera extract with the copper and zinc salts was used for the synthesis of CuO and CuZnO nanoparticles. Consequently, metal ions were reduced. The phytochemicals such as phenolic compounds, flavonoids and glycosides played crucial roles in the stabilization of nanoparticles as well as in the enhancement of bioactivity. The reduction of Cu2+ and Zn2+ ions through bio synthesis produced well-defined stable nanoparticles. The methodology is green, as it does not require toxic reagents, and constitutes an efficient and benign approach for the non-toxic synthesis of metal oxide nanoparticles for e.g. photocatalytic and antimicrobial applications. (22,23,24,25)

3.1 X-ray diffraction (XRD)

X-ray diffraction (XRD) investigation validated the effective production and crystallinity of CuO and CuZnO nanoparticles. XRD analysis revealed that the calculated diffraction peaks corresponding to CuO nanoparticles were directly related to the monoclinic CuO phase (JCPDS 01-089-5899), showing dominant peaks at (110) and (002) with 29.40° and 35.60° respectively. By comparison with the XRD pattern of CuO (JCPDS card No. 45-0937) and Cu/ZnO (JCPDS card No. 36-1451), the CuZnO nanoparticles gave rise to the additional diffraction peaks at 16.79°, 39.70°, and 48.50° respectively, which suggested that Zn ions were incorporated into the CuO lattice. Successful Zn doping was also confirmed by the minor 2θ values shift along with d-spacing changes. CuO nanoparticles exhibited a crystallite size of 20.2 nm and CuZnO nanoparticles exhibited a similar crystallite size of 20.8 nm. (26)

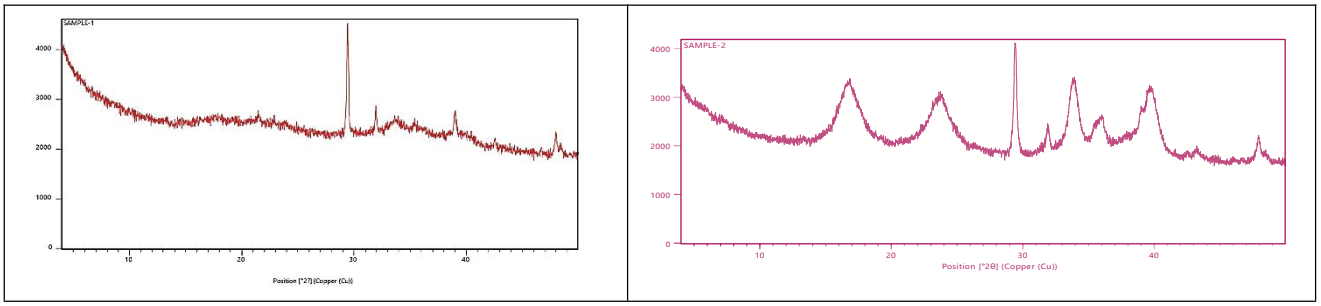

Fig.3 XRD Pattern of the green synthesized CuO (Sample 1) and CuZnO (Sample-2)

3.2 Ultraviolet-visible spectroscopy

UV-Vis absorption spectra of CuO nanoparticles exhibited a strong absorption peak around 320–350 nm, characteristic of CuO, and a wide absorption peak at 500–700 nm, indicating agglomeration or mixed oxidation states. CuO exhibited a semiconductive characteristic, with Eg value ranging from 1.7–2.1 eV. Absorption spectra of the CuZnO nanoparticles displayed an absorption peak at approximately 350–380 nm, which was also considerably redshifted, as compared to that of pure ZnO (360 nm), confirming that Cu was integrated in the lattice of ZnO. The displayed prolonged absorption into the visible spectrum can be argued to stem from improved photocatalytic activity due to cu doping. The band gap of CuZnO was found to be approximately 2.5 and 3.1 eV. smaller than that of pure ZnO (3.3 eV), implying an alteration in the electronic structure to enhance the photocatalytic efficiency. (27).

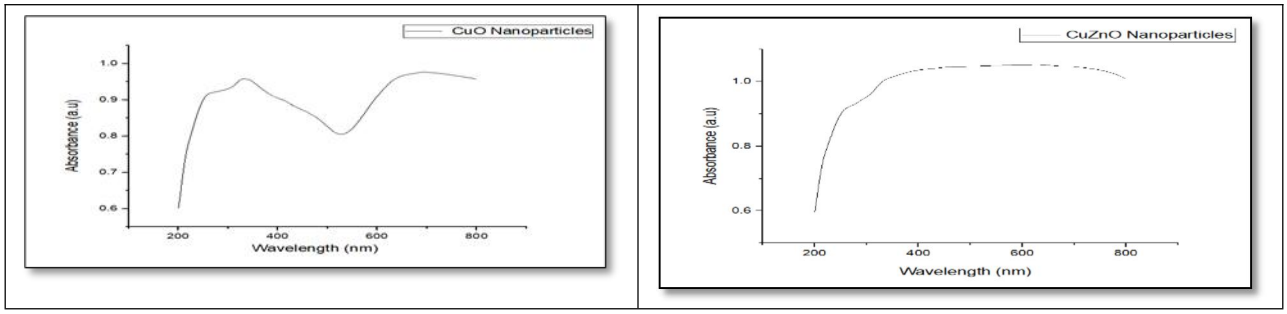

Fig.4 UV-Vis Spectroscopy Absorbance Peak of Copper oxide (CuO) and copper Zinc Oxide (CuZnO) nanoparticles

3.3 FTIR Study

FTIR spectra demonstrating distinctive function group absorption peaks verified the effective production of CuO and CuZnO nanoparticles. The large peak in the 3522 cm^{-1} range for CuO nanoparticles in Fig. 3C matched hydroxyl (-OH) functional groups, which might have come from adsorbed water or plant biomolecules. Peaks at 1844 cm^{-1} and 1638 cm^{-1} connected to the C=O stretching and H-O-H bending demonstrated the presence of water on the surface. The formation of pure CuO nanoparticles was evidenced through the observation of C-O stretching at 1421 cm^{-1}° and intense Cu-O stretching peaks at 1051 cm^{-1}, 701 cm^{-1}, and 419 cm^{-1}. For CuZnO nanoparticles, the FTIR spectra revealed a broad band centred at 3200–3600 cm^{-1} that was ascribed to hydroxyl (−OH) groups, whereas for organic residues, the peaks at 2927 cm^{-1} and 2856 cm^{-1} corresponded to C−H stretching. The absorption peaks found at 1749 cm^{-1} (C=O) confirmed the presence of Amide I, II, and the formation of a C=O functional group. This is because the keratin molecules' C=O bond stretching mode changed from α-helix to more β-conformation based on the cross-b recovery of the protein bodies folding. Peak intensities at 1132 cm^{-1}, 931 cm^{-1}, 620 cm^{-1}, and 500 cm^{-1} are strong and attributed to Cu-O and Zn-O stretching vibrations indicating that Zn was incorporated into the CuO lattice. (28)

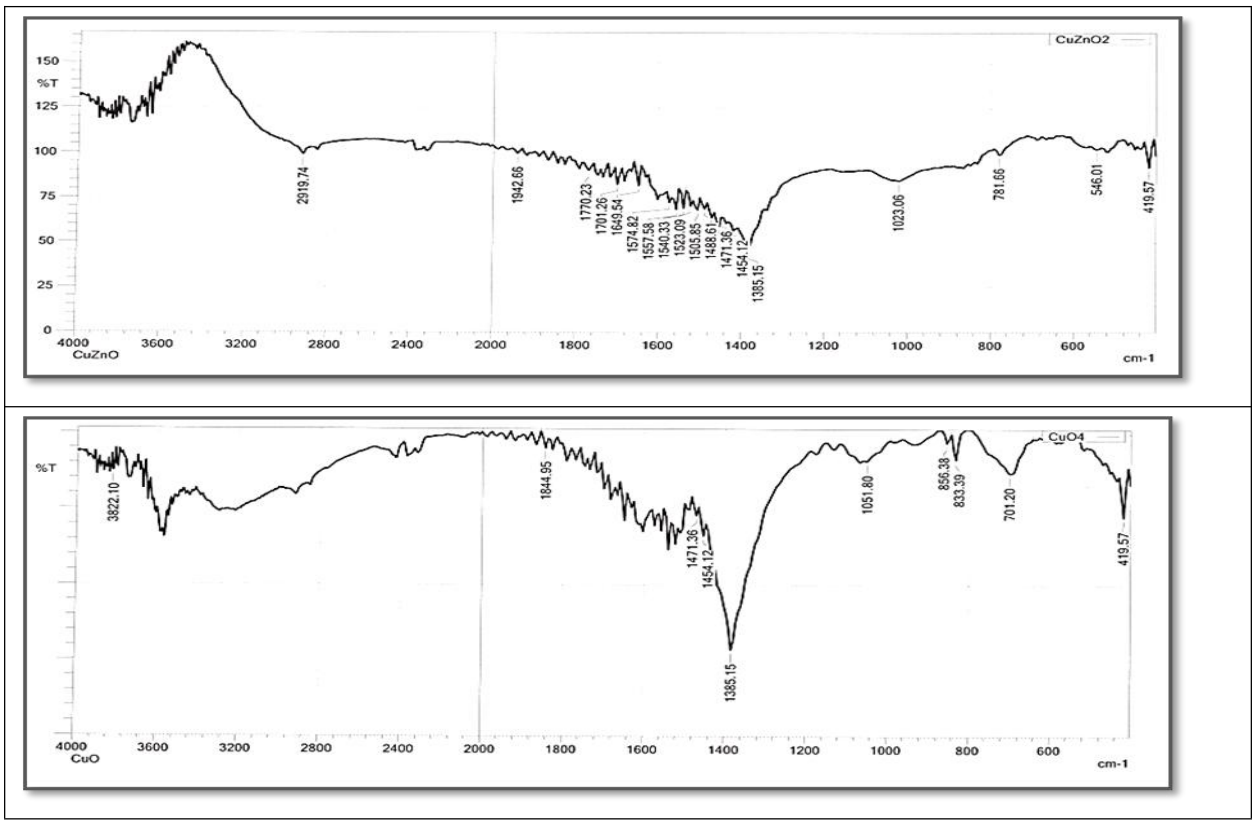

Fig.5 FTIR Spectra of Copper oxide (CuO) and copper Zinc Oxide (CuZnO) nanoparticles

3.4 SEM Analysis

The effective fabrication of spherically shaped CuO and CuZnO nanoparticles is evident from the SEM pictures. Due to improved functional characteristics brought about by increased surface roughness and porosity, CuZnO had a more uniform dispersion than CuO. By using energy-dispersive spectroscopy (EDS) analysis, the elemental composition was

verified. (Fig7, Fig8), which showed the expected Cu and O in CuO and additional Zn peaks in CuZnO, confirming successful Zn incorporation. The presence of no impurity indicated high purity, indicating that these nanoparticles could be an eco-friendly cardio-protective agent for photocatalysis and anti-bacterial activity. (29)

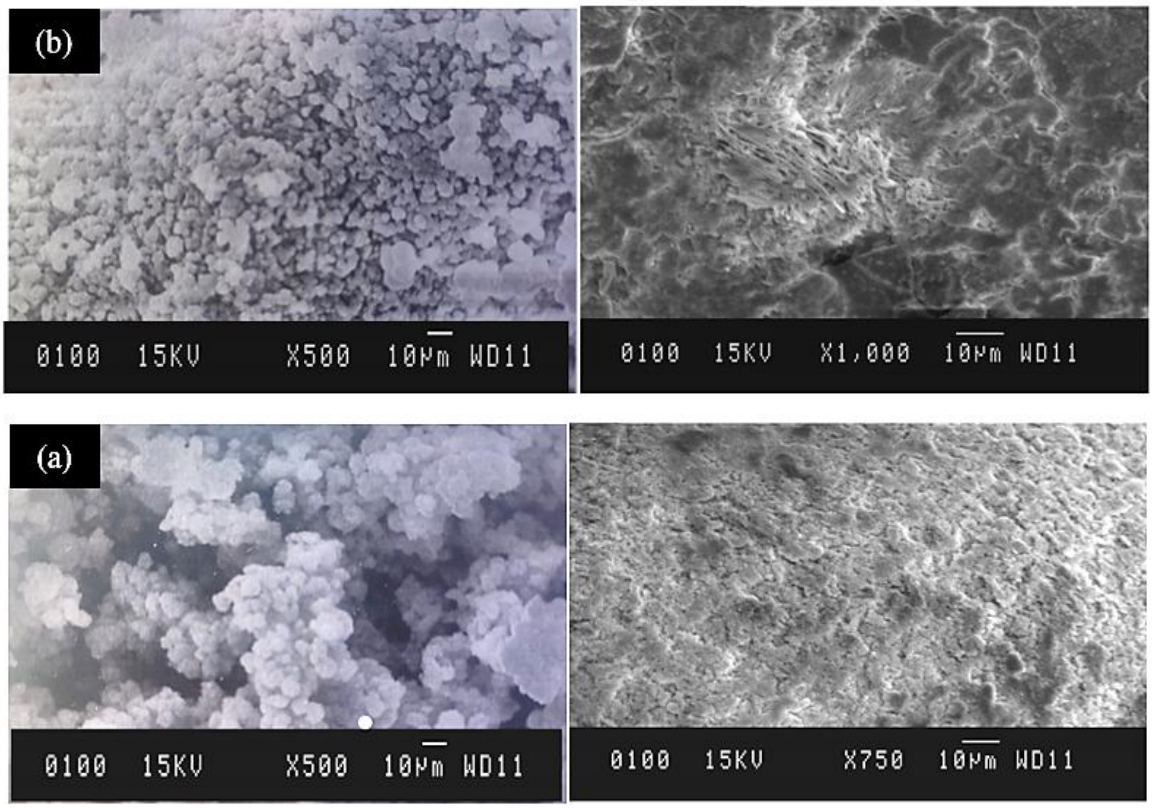

Fig.6 SEM image for (a) CuO and CuZnO NPs

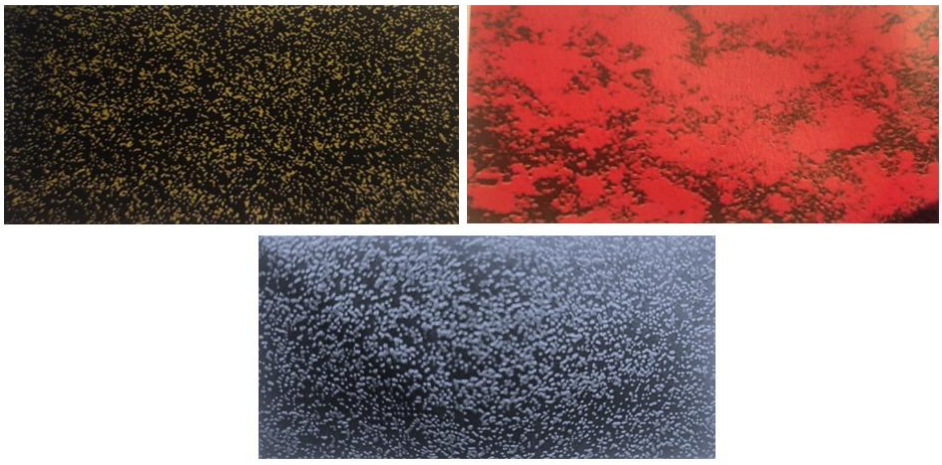

Fig7: EDS Mapping of copper oxide nanoparticles

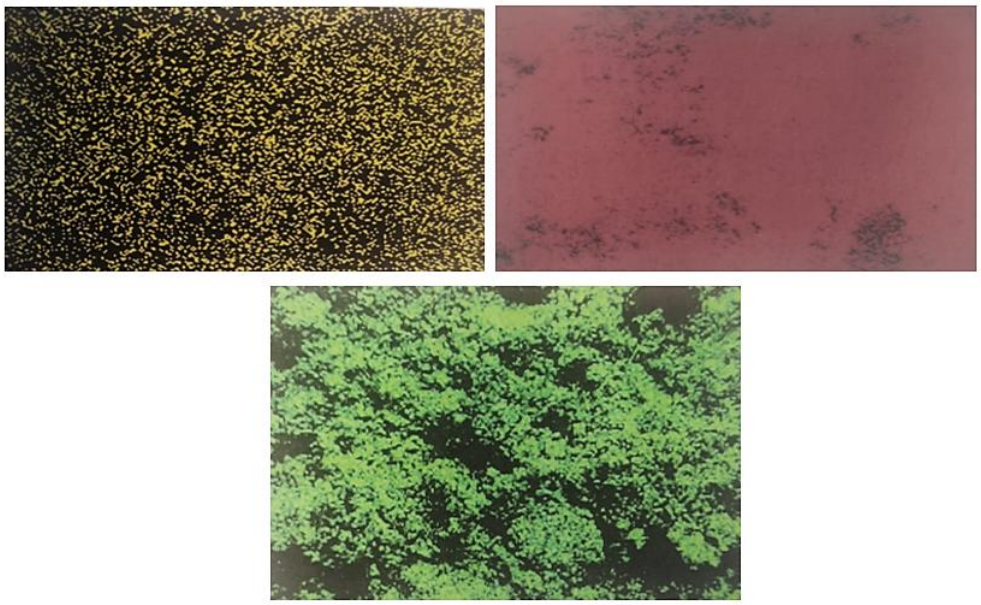

Fig8: EDS Mapping of copper Zinc oxide nanoparticles

3.5 TEM Analysis

TEM analysis confirmed the spheroidal morphology of CuO and CuZnO nanoparticles, with CuO being smaller (8 ± 0.19 nm) than CuZnO (15 ± 0.73 nm). The size variation is attributed to biomolecules used in synthesis. Their well-defined morphology enhances catalytic and biomedical applications.

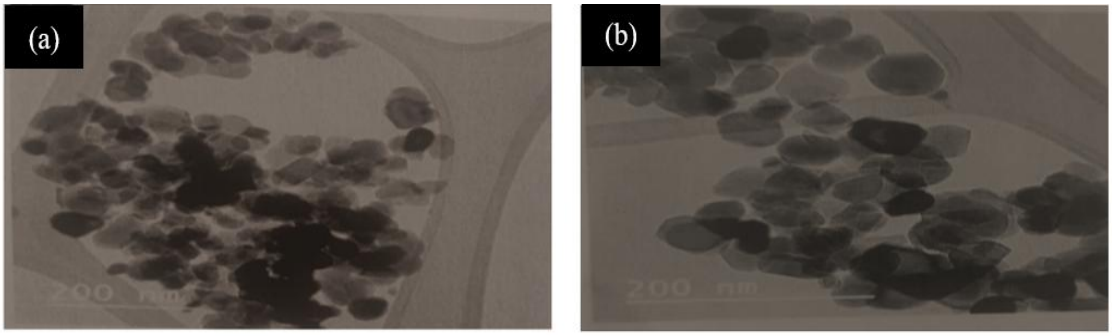

Fig.9 TEM images for (a) CuO and (b) CuZnO NPs

3.6 Antibacterial activity

The smaller-size nanoparticles of CuO and CuZnO (19-21 nm) showed more zone of inhibition against E. coli which was confirmed with well diffusion method. In fact, CuZnO showed more inhibition than CuO, with the zones of inhibition (ZOI) were 24 mm, 29 mm, and 33 mm for CuO 5, 10, and 20 mg/mL, respectively. In the case of CuZnO, similar observations were found with higher ZOIs of 26 mm, 30 mm, and 33 mm at the respective concentrations. These results suggest that smaller NPs infiltrate bacterial membranes more readily, illuminating them as potential candidates for antimicrobial applications including food wrapping and biomedical coatings.

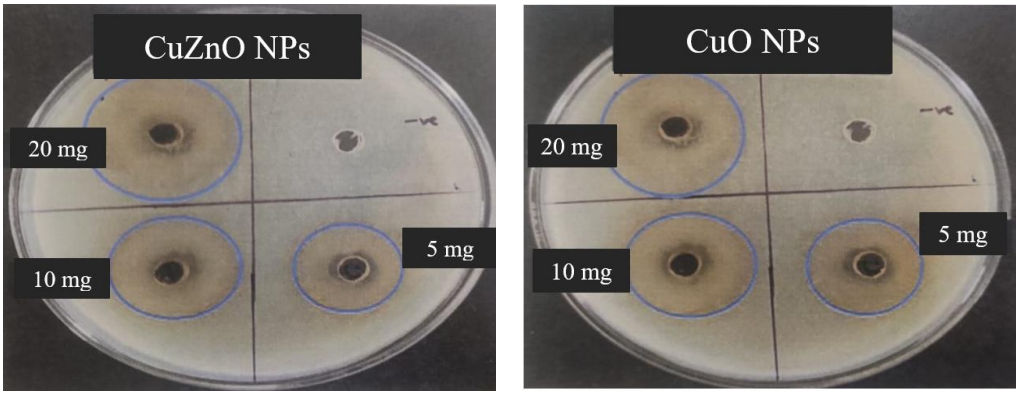

Fig.7 ZOI against Escherichia coli bacteria for CuO and CuZnO NPs

3.7 Photocatalytic analysis

According to a prior work, CuO and CuZnO nanoparticles have a wide absorption spectrum and are excellent photocatalysts for the efficient photocatalytic degradation of Malachite Green (MG) dye after 80 minutes of UV light irradiation. The degradation of MG dye without nanoparticles was only 8.453%, while the stability and efficiency of degradation were greatly improved by using CuO and CuZnO, with the maximum reaching up to 95%. This resulted in a direct relationship between catalyst content and degradation rate, since higher concentrations produced greater efficiency. The formation of electron-hole pairs by UV absorption was conducive to the degradation of dye molecules, and the tiny size and wide surface area of the nanoparticles boosted the photocatalytic activity. High R^2 regression coefficient values confirmed that the process followed a monolayer adsorption mechanism, and the kinetic data fit well to pseudo-first-order kinetic model. The results suggest that CuO and CuZnO nanoparticles could be useful photocatalysts for wastewater treatment applications.

Table no 3.3: Regression coefficient and degradation efficiency (%) of MG dye utilizing CuO and CuZnO NPs

Dye	NPs	Concentrations (mg)	Degradation (%)	Rate Constant (Min-1)	Regression Coefficient
MG (Without NPs)	-	-	8.453	-	-
MG	CuO	25	85.994	0.00243	0.95597
		50	88.327	0.00211	0.96824
		100	91.836	0.00263	0.95479
	CuZnO	25	88.919	0.00285	0.95245
		50	92.995	0.00212	0.97367
		100	95.127	0.00173	0.98309

4. CONCLUSION

In this study, CuO and CuZnO NPs were successfully synthesized using a green method in the presence of Moringa oleifera extract and they characterized structurally, optically, antibacterial and photocatalytic properties. The formation of high crystalline nanoparticles with unique morphological and functional properties were characterized by XRD, FTIR, UV-Vis, SEM, and TEM. These characterizations revealed the crystalline nature of CuO and provided evidence for a successful incorporation of zinc into the CuO lattice, while in the FTIR spectra, different peaks correlated to biomolecules that aided in stabilizing the nanoparticles were observed. SEM and TEM images revealed spherical morphology, and CuZnO was found more uniform and evenly distributed than CuO. The means of monitoring antibacterial activity using the well diffusion technique confirmed substantial inhibition of E. coli, while CuZnO presented larger inhibition halo versus CuO, indicating enhanced antibacterial efficiency owing to synergistic effects. According to a pseudo-first-order

kinetic model, CuZnO demonstrated a significant degradation efficiency of 95% at elevated concentrations, and XRD analysis verified the formation of a hexagonal crystalline structure. The photocatalytic degradation of Malachite Green (MG) dye was optimal under UV irradiation. Increased surface area, suitable band gap characteristics, and efficient electron-hole pair formation were the outcomes of this. Overall, the study's findings indicate that CuO and CuZnO nanoparticles may have excellent antibacterial qualities and be used in medicinal and environmental applications through photocatalysis. With their environmentally friendly synthesis, high purity, and multifunctionality, these gems are potential contenders in wastewater treatment, antimicrobial coatings, and other nanotechnology-based applications. Further possible optimization and applicability in wastewater treatment systems can investigate scalability, as well as biomedical applications as they relate to the respective function of these novel compounds.

REFERENCES

[1] R. Shashanka, Jayaprakash, G. K., Prakashaiah, B. G., Kumar, M., & Kumara Swamy, B. E. (2022). Electrocatalytic determination of ascorbic acid using a green-synthesised magnetite nano-flake modified carbon paste electrode by cyclic voltammetric method. *Materials Research Innovations*, 1-11. https://doi.org/10.1080/14328917.2021.1945795

[2] Shashanka, R., & Ceylan, K. B. (2020). The activation energy and antibacterial investigation of spherical Fe_3O_4 nanoparticles prepared by *Crocus sativus* (Saffron) flowers. *Biointerface Research in Applied Chemistry, 10*(4), 5951-5959. https://doi.org/10.33263/BRIAC104.951959

[3] Shashanka, R., Abdullah Cahit, K., Yusuf, C., & Orhan, U. (2020). A fast and robust approach for the green synthesis of spherical magnetite (Fe_3O_4) nanoparticles by *Tilia tomentosa* (Ihlamur) leaves and its antibacterial studies. *Pharmaceutical Sciences, 26*(2), 175-183. https://doi.org/10.23893/1307-2080.APS.05915

[4] W. Ahmad, S.C. Bhatt, M. Verma, V. Kumar, H. Kim A review on current trends in the green synthesis of nickel oxide nanoparticles, characterizations, and their applications Environ. Nanotechnol. Monit. Manag., 18 (2022), p. 100674

[5] M. Pirhashemi, A. Habibi-Yangjeh, S. Rahim Pouran Review on the criteria anticipated for the fabrication of highly efficient ZnO-based visible-light-driven photocatalysts J. Ind. Eng. Chem., 62 (2018), pp. 1-25

[6] H. Agarwal, S. Venkat Kumar, S. Rajeshkumar A review on green synthesis of zinc oxide nanoparticles – an eco-friendly approach Resour.-Eff. Technol., 3 (2017), pp. 406-413

[7] W. Ahmad, A. Pandey, V. Rajput, V. Kumar, M. Verma, H. Kim Plant extract mediated cost-effective tin oxide nanoparticles: a review on synthesis, properties, and potential applications Curr. Res. Green Sustain. Chem., 4 (2021), p. 100211

[8] W. Ahmad, D. Kalra, Green synthesis, characterization and anti-microbial activities of ZnO nanoparticles using Euphorbia hirta leaf extract J. King Saud Univ. Sci., 32 (2020), pp. 2358-2364

[9] Azizi-Lalabadi, M., Ehsani, A., Alizadeh-Sani, M., & Divband, B. (2019). Antibacterial activity of titanium dioxide and zinc oxide nanoparticles biosynthesized by *Lactobacillus plantarum* against *Pseudomonas aeruginosa* and *Staphylococcus aureus*. *Scientific Reports*, 9, 13630.

[10] Xia, X., Wang, Y., Ruditskiy, A., & Xia, Y. (Funabiki). 25th Anniversary Article: Galvanic Replacement: A Versatile Route to Hollow Nanostructures with Tunable and Well-Controlled Properties. *Advanced Materials*, 28(45), 10517–10528. https://doi.org/10.1002/adma.201601291

[11] Ahmed, S., Annu, Ikram, S., & Yudha, S. S. (2023). Plant-Based Copper Oxide Nanoparticles; Biosynthesis, Characterization and Their Antimicrobial Activities. *Catalysts*, 13(2), 348. https://doi.org/10.3390/catal13020348

[12] Gadewar, M., Prashanth, G. K., Babu, M. R., Dileep, M. S., Prashanth, P., Rao, S., & Mahadevaswamy, M. (2024). Unlocking nature's potential: Green synthesis of ZnO nanoparticles and their multifaceted applications - A concise overview. *Journal of Saudi Chemical Society*, 28(1), 101774. https://doi.org/10.1016/j.jscs.2023.101774

[13] Yin et al., 2015 Hameed, A. S. H., Karthikeyan, C., Ahamed, A. P., Thajuddin, N., Alharbi, N. S., Alharbi, S. A., & Ravi, G. (2016). In vitro antibacterial activity of ZnO and Nd doped ZnO nanoparticles against ESBL producing Escherichia coli and Klebsiella pneumoniae. *Scientific Reports*, 6, 24312. https://doi.org/10.1038/srep24312

[14] Kashyap, P., Kumar, S., Riar, C.S., Jindal, N., Baniwal, P., Guiné, R.P.F., Correia, P.M.R., Mehra, R., & Kumar, H. (2022). Recent Advances in Drumstick (*Moringa oleifera*) Leaves Bioactive Compounds: Composition, Health Benefits, Bioaccessibility, and Dietary Applications. *Antioxidants*, 11(2), 402. https://doi.org/10.3390/antiox11020402

[15] Gupta et al., 2023). Gupta, R., Kuppusamy, P., & Doss, C. G. P. (2023). Moringa oleifera: An updated comprehensive review of its pharmacological activities, phytochemistry, and ethnomedicinal uses. *International Journal of Molecular Sciences*, 24(3), 2098. https://doi.org/10.3390/ijms24032098

[16] Sahoo, S., Gedefaw, D., & Mitiku, M. (2020). Carbon sequestration potential of *Moringa oleifera* in the drylands of Ethiopia. *Cogent Environmental Science*, 6(1), 1778996. https://doi.org/10.1080/23311843.2020.1778996

[17] Singh, A., et al. (2023). Moringa oleifera Lam.: A comprehensive review on active ingredients, pharmacological activities, applications in food and cosmetics industries and safety considerations. *RSC Advances*, 13, 290–310. https://doi.org/10.1039/D3RA03584K

[18] W. Ahmad, K.K. Jaiswal, S. Soni Green synthesis of titanium dioxide (TiO2) nanoparticles by using Mentha arvensis leaves extract and its antimicrobial properties Inorg Nano-Met. Chem. (2020), 10.1080/24701556.2020.1732419

[19] W. Ahmad, S. Singh, S. Kumar Phytochemical Screening and antimicrobial study of Euphorbia hirta extracts J. Med. Plants Stud., 5 (2) (2017), pp. 183-186

[20] Saleh, M. M. A., Ali, T. M. M., & Ali, R. M. Q. (2023). Synthesis and characterization of copper oxide nanoparticles using Moringa oleifera leaves extract. *University of Aden Journal of Natural and Applied Sciences*, 27(2), 335–345. https://doi.org/10.47372/uajnas.2023.n2.a14

[21] Das, P. E., Abdul, S. N., Al-Yousef, I. A., & Mohammed, A. F. (2020). Green synthesis of encapsulated copper nanoparticles using a hydroalcoholic extract of Moringa oleifera leaves and assessment of their antioxidant and antimicrobial activities. *Molecules*, 25(3), 555. https://doi.org/10.3390/molecules25030555

[22] R. Shashanka, P. Taslimi, A.C. Karaoglanli, O. Uzun, E. Alp, G. KudurJayaprakashe Photocatalytic degradation of Rhodamine B (RhB) dye in wastewater and enzymatic inhibition study using cauliflower shaped ZnO nanoparticles synthesized by a novel One-pot green synthesis method Arab. J. Chem., 14 (6) (2021), p. 103180

[23] R. Shashanka Investigation of optical and thermal properties of CuO and ZnO nanoparticles prepared by Crocus Sativus (Saffron) flower extract J. Iran. Chem. Soc., 18 (2) (2021), pp. 415-427

[24] R. Shashanka, B.E. Kumaraswamy Biosynthesis of silver nanoparticles using leaves of Acacia melanoxylon and their application as dopamine and hydrogen peroxide sensors Phys. Chem. Res., 8 (1) (2020), pp. 1-18

[25] R. Shashanka, V.M. yilmaz, A.C. Karaoglanli, O. Uzun Investigation of activation energy and antibacterial activity of CuO nano-rods prepared by Tilia Tomentosa (Ihlamur) leaves Moroc. J. Chem., 8 (2) (2020), pp. 497-509

[26] S. Noreen, G. Mustafa, S.M. Ibrahim, S. Naz, M. Iqbal, M. Yaseen, T. Javed, J. Nisar Iron oxide (Fe2O3) prepared via green route and adsorption efficiency evaluation for an anionic dye: kinetics, isotherms and thermodynamics studies J. Mater. Res. Technol., 9 (2020), pp. 4206-4217, 10.1016/j.jmrt.2020.02.047

[27] M.-C. María, L.-C. Marta, J.L. Barriada, H. Roberto, E. Manuel, de V. Sastre, Green synthesis of iron oxide nanoparticles. Development of magnetic hybrid materials for efficient as (V) removal, Chem. Eng. J. 301 (2016) 83–91.

[28] C.P. Devatha, T. Arun Kumar, K. Swetha, Green synthesis of Iron Nanoparticles using different leaf extracts for treatment of domestic wastewater, J. Clean. Prod. 139 (2016) 1425–1435.

[29] A.A. Khaleel, Nanostructured Pure c-Fe2O3 via forced precipitation in an organic solvent, Chem. Eur J. 10 (2004) 925–932.